Published in final edited form as:
Am J Physiol Endocrinol Metab. 2005 December ; 289(6): E1077–E1084.

Decreased insulin-dependent glucose transport by chronic ethanol feeding is associated with dysregulation of the Cbl/TC10 pathway in rat adipocytes

Becky M. Sebastian and **Laura E. Nagy**
Department of Nutrition, Case Western Reserve University School of Medicine, Cleveland, Ohio, 44106

Abstract

Heavy alcohol consumption is an independent risk factor for type 2 diabetes. While the exact mechanism by which alcohol contributes to the increased risk is unknown, impaired glucose disposal is a likely target. Insulin-stimulated glucose disposal in adipocytes is regulated by two separate and independent pathways: the PI3K pathway and the Cbl/TC10 pathway. Previous studies suggest that chronic ethanol feeding impairs insulin-stimulated glucose transport in adipocytes in a PI3K-independent manner. In search of potential targets of ethanol that would affect insulin-stimulated glucose transport, we investigated the effects of 4-week ethanol feeding to male Wistar rats on the Cbl/TC10 pathway in isolated adipocytes. Chronic ethanol feeding inhibited insulin-stimulated cCbl phosphorylation compared to pair-feeding. Insulin receptor and Akt/PKB phosphorylation were not affected by ethanol feeding. Chronic ethanol exposure also impaired cCbl and TC10 recruitment to a lipid raft fraction isolated from adipocytes by detergent extraction. Furthermore, chronic ethanol feeding increased the amount of activated TC10 and filamentous actin in adipocytes at baseline, and abrogated the ability of insulin to further activate TC10 or polymerize actin. These results demonstrate that the impairment in insulin-stimulated glucose transport observed in adipocytes after chronic ethanol feeding to rats is associated with a disruption of insulin-mediated Cbl/TC10 signaling and actin polymerization.

Keywords

lipid raft; cCbl; TC10; GTPase; actin polymerization; glucose metabolism; insulin resistance

INTRODUCTION

Type 2 diabetes, a metabolic disease prevalent in the United States and other westernized countries, is characterized by chronic hyperglycemia caused by insulin resistance. Risk factors for type 2 diabetes include family history, overnutrition, obesity, inactivity, and abstinence or heavy consumption of alcohol. The association between alcohol consumption and type 2 diabetes is complex; studies have demonstrated a U-shaped relationship where moderate drinkers have a decreased risk for type 2 diabetes, while non-drinkers have increased risk, and heavy drinkers have the greatest risk (22;54;56). The exact mechanism by which heavy alcohol consumption leads to type 2 diabetes is unknown. However, disruptions in carbohydrate and glucose metabolism with ethanol exposure likely contribute to the increased risk (2. In

Correspondence to: Laura E. Nagy.

Address correspondence to: Laura E. Nagy, Department of Nutrition, Case Western Reserve University, 10900 Euclid Ave., Cleveland, Ohio, 44106-4906, Tel. 216 368-6230; Fax. 216 368-6644; E-Mail: len2@case.edu.

The work in this study was supported by NIH AA 11876.

particular, ethanol exposure leads to the development of insulin resistance and impaired glucose disposal, characterized by elevated fasting blood glucose levels (19;46) and non-fasting hyperglycemia (9.

Muscle and adipose tissue are the major sites of glucose disposal in response to insulin. In these tissues, the phosphatidylinositol 3-kinase (PI3K)[1] pathway regulates the translocation of the insulin-responsive glucose transporter, GLUT4, from intracellular pools to the plasma membrane (PM). Insulin activates the tyrosine kinase activity of the insulin receptor leading to autophosphorylation of the insulin receptor on several tyrosine residues and the phosphorylation of the insulin receptor substrate 1 (IRS1) (27). The phosphorylated IRS1 becomes a target for the regulatory subunit of PI3K, p85, activating the PI3K catalytic subunit p110 (35). The activation of PI3K leads to the downstream phosphorylation of Akt/PKB and atypical PKCξ, both shown to play a role in translocation of GLUT4 to the PM and glucose uptake (3;4;8;25;50;53).

While the PI3K pathway is necessary for insulin-stimulated glucose uptake, several lines of evidence suggest this pathway alone is insufficient to mediate uptake (11;14;17;26;30;37;49; 57) and are reviewed in (45). A second insulin-signaling cascade implicated in glucose transport is the Cbl/TC10 pathway. In response to insulin, APS (adapter protein with pleckstrin homology (PH) and Src homology 2 (SH2) domains) is recruited to the autophosphorylated insulin receptor and binds via its SH2 domain (1;28). APS is phosphorylated by the insulin receptor at Y618 (34), which becomes a docking site for the adapter protein cCbl. cCbl is found in the cytosol constitutively bound to the Cbl-associated protein (CAP) (28). Once associated with APS, the insulin receptor phosphorylates cCbl (28). This phosphorylation provides a binding site for the protein CrkII (44). CrkII is localized in the cytosol and is bound to C3G, a guanylnucleotide exchange factor (GEF) (24). These proteins are recruited to lipid raft microdomains of the plasma membrane after insulin stimulation (5;23). Also present in the lipid raft, is the Rho family GTPase, TC10. C3G can function as a GEF for TC10, resulting in its activation. Studies utilizing dominant negative forms of CAP and TC10 implicate the Cbl/ TC10 pathway in cortical actin polymerization/rearrangement, exocyst complex recruitment and maximal glucose transport in response to insulin (6). A recent study argues against a role for Cbl/TC10 in insulin-stimulated glucose uptake in muscle cells (16). Further, arecent study using siRNA strategies argues against TC10's involvement in insulin-stimulated glucose uptake in 3T3L1 adipocytes (33).

Chronic ethanol feeding in rats decreases insulin-stimulated glucose transport and decreases GLUT4 surface-accessibility in isolated adipocytes (41;58), but does not impair the association of the p85 subunit of PI3K with tyrosine phosphorylated proteins or the serine phosphorylation of Akt/PKB (41). These data suggest that ethanol impairs insulin-stimulated glucose transport in adipocytes in a PI3K-independent manner. In search of potential targets of ethanol that could impair insulin-stimulated glucose transport, we focused on the PI3K-independent Cbl/TC10 pathway. Here we show chronic ethanol feeding decreased insulin-stimulated cCbl phosphorylation and its recruitment to the lipid raft. Further, chronic ethanol feeding disrupted the critical cycle of GTP loading/GTP hydrolysis of TC10 by increasing activation of TC10 in the absence of insulin, and preventing further activation in response to insulin. Chronic ethanol feeding also impaired insulin-stimulated actin polymerization, shown in other studies to be regulated by TC10 (18). These data demonstrate that impaired glucose disposal in adipocytes after chronic ethanol exposure is associated with a disruption in the Cbl/TC10 pathway at multiple sites.

[1]The abbreviations used are: PI3K, phosphatidylinositol 3-kinase; PKB, protein kinase B; GLUT4, glucose transporter 4; PM, plasma membrane; IRS1, insulin receptor

EXPERIMENTAL PROCEDURES

Materials

Male Wistar rats weighing 170-180g were purchased from Harlan Sprague Dawley (Indianapolis, IN). Lieber DeCarli ethanol diet was purchased from Dyets (Bethlehem, PA). Antibodies were obtained from the following sources: anti-phospho-tyrosine (PY100), anti-phospho-Akt/PKB (Ser473), anti-Akt/PKB, and anti-APS from Cell Signaling Technology (Beverly, MA); anti-cCbl, and anti-insulin receptor β subunit from Santa Cruz (Santa Cruz, CA); anti-phospho-tyrosine (4G10) from Upstate (Charlottesville, VA); anti-TC10 from Affinity BioReagents (Golden, CO); anti-transferrin receptor from Zymed (South San Francisco, CA); anti-caveolin-1 from BD Transduction Laboratories (San Jose, CA); anti-actin from Cytoskeleton, Inc. (Denver, CO). Maltose dextrin was purchased from BioServ (Frenchtown, NJ), Immunopure® immobilized protein G agarose beads from Pierce Biotechnology Inc. (Rockford, IL), Complete™, EDTA-free protease inhibitor cocktail tablet and enhanced chemiluminescence reagent from Roche (Indianapolis, IN), the cdc42 activation assay kit from Upstate (Charlottesville, VA), and all other reagents were purchased from Sigma (St. Louis, MO).

Animal Feeding and Adipocyte Isolation

The chronic ethanol feeding model used in this study has been previously described (43). Briefly, upon arrival, rats were acclimated to their environment for 3 days, and then introduced to a liquid diet for 2 days. Randomly-selected rats assigned to the ethanol-fed group were provided an *ad libitum* liquid diet containing ethanol as 35% of total caloric value for four weeks. Control rats were pair-fed a liquid diet with maltose dextrin isocalorically substituted for ethanol. All animal procedures were approved by the Institutional Animal Care and Use Committee at Case Western Reserve University. After the four-week ethanol feeding, rats were anesthetized by intraperitoneal injection with 0.075 (ethanol-fed rats) or 0.12 mL (pair-fed rats)/100 g body weight of a cocktail containing 10 mg/mL Acepromazine, 100 mg/mL Ketamine and 20 mg/mL Xylazine and epididymal fat pads removed. Adipocytes were isolated by collagenase digestion as previously described, except that bovine serum albumin (BSA) was excluded from the wash buffer (58). Isolated adipocytes were counted and adjusted to a cell density of 2×10^6 cells/mL, unless otherwise noted.

Immunoprecipitation and Western Blotting

Four mL of isolated adipocytes were incubated with or without 10 nM insulin for 0-1.5 min at 37°C in a shaking water bath (100 rpm) and then immediately placed on ice and lysed in 1% Triton X-100 lysis buffer (50 mM Tris, 6.4 mM NaCl, 1 mM EDTA, 1mM Na pyrophosphate, 1mM activated Na vanadate, 10 mM NaF, and protease inhibitor cocktail at 1 Complete™ tablet/2.6 mL) for 30 min. Lysates were centrifuged in a micro-centrifuge 3 min at 4000×g at 4°C and the infranatant removed and assayed for protein content. Three milligrams of protein from each sample was incubated with 6 μg anti-cCbl antibody rotating overnight at 4°C and then 2.5-3 hour incubation rotating at 4°C with 50 μL protein G agarose beads. Immune complexes were pelleted in a micro-centrifuge 5 min at 500×g at 4°C, followed by 2 washes with ice-cold PBS (rotated at 4°C for 15 min for each wash). The final pellet was resuspended in 40 μL Laemmli buffer (30 mM Tris, pH 6.8, 5% glycerol, 1% SDS, 2.5% β-mercaptoethanol, and 0.125 mg/mL bromophenol blue). All samples were boiled 5 min prior to loading on a 6% SDS-polyacrylamide gel and transferred to PVDF membrane using a semi-dry transfer technique with continuous transfer buffer according to standard protocols. All blots were blocked with 3% BSA in Tris buffered saline pH 7.6 containing 0.1% Tween-20 prior to overnight incubation at 4°C with primary antibodies. After one hour incubation with secondary antibody and subsequent washes, bound antibodies were visualized using enhanced chemiluminescence reagent. Films were scanned and the densities of immunoreactive protein

were analyzed on a Macintosh computer using the public domain NIH Image program (developed at the U.S. National Institutes of Health and available on the Internet at http://rsb.info.nih.gov/nih-image/); film exposure times were in the linear range of detectability.

Plasma Membrane Isolation

Isolated adipocytes were counted and adjusted to a cell density of 1×10^6 cells/mL and were incubated with or without 10 nM insulin for 0-5 min at 37°C in a shaking water bath (100 rpm). Stimulation was terminated with 2mM KCN and cells were immediately placed on ice. Plasma membrane fractions were obtained by differential centrifugation as previously described (41) with few exceptions. Briefly, cells were homogenized in 500 μL, 10 strokes in a glass-on-glass dounce with a loose-fitting pestle, and homogenates were centrifuged 15,000×g, 15 min at 4° C. Pellets were washed with 1mL homogenization buffer (20 mM Tris, pH 7.4, 1 mM EDTA, and 255 mM sucrose with added protease inhibitor cocktail at 1 Complete™ tablet/50 mL buffer) and resuspended in 500 μL homogenization buffer and layered over a sucrose pad (20 mM Tris, pH 7.4, 1 mM EDTA, and 1.12 M sucrose) and centrifuged 100,000×g for 70 min. The interface was collected and centrifuged 16,000×g, 15 min at 4°C. Pellets (isolated PM) were resuspended in 50 μL homogenization buffer and assayed for protein content.

Preparation of Triton-Insoluble Fraction

Caveolin-enriched, Triton-insoluble fractions were obtained using a technique adapted from Mastick and Saltiel (31). Isolated adipocytes (1-4 mL) were incubated with or without 10 nM insulin for 0-5 min at 37°C in a shaking water bath (100 rpm), immediately placed on ice, and lysed 30 min rocking at 4°C in 1% Triton X-100 lysis buffer (5 mM Tris pH 7.4, 15 mM NaCl, 1.6 mM EGTA, 2 mM Na pyrophosphate, 1 mM activated Na vanadate, 10 mM NaF, 1 mM benzamadine, 1 mM molybdenum, and protease inhibitor cocktail at 1 Complete™ tablet/500 mL buffer). Lysates were homogenized at 4°C in a glass homogenizer with a tight-fitting pestle, 10 strokes and then centrifuged in a micro-centrifuge 2 min, 250×g to remove nuclei and float triglycerides. Infranatants were centrifuged 20 min at 15,000×g to separate Triton-soluble material from Triton-insoluble pellets. Pellets were washed with 1% Triton X- 100 lysis buffer and the final pellet was resuspended by vortexing and triturating with 60 mM octyl β-D-thioglucopyranoside (OTG), dissolved in 1% Triton X-100 lysis buffer. All samples were normalized for protein prior to Western analysis. Triton-insoluble and soluble fractions of PM were prepared by incubating isolated PM in the 1% Triton X-100 lysis buffer for 30 min, rotating at 4°C and then centrifuged at 15,000×g for 20 min to separate Triton-soluble material from Triton-insoluble pellets.

TC10 Activation Assay

One milliliter of isolated adipocytes at 1×10^6 cells/mL were incubated with or without 10 nM insulin for 0-5 min at 37°C in a shaking water bath (100 rpm). Active TC10 levels were measured using a GST pull-down assay kit following the manufacturer's instructions. Briefly, cells were lysed using a Mg^{2+} lysis buffer (MLB, provided in kit), cellular debris removed by centrifugation (5 min at 14,000×g, 4°C), and lysates were incubated with PAK-1 PBD-coupled agarose beads which bind GTP-bound GTPases, for 45 min at 4°C, with gentle agitation. Complexes were pelleted (10 sec at 14,000×g, 4°C), washed 3 times with MLB, resuspended in 40 μL of 2X Laemmli buffer and boiled 5 minutes. Agarose beads were removed by centrifugation (10 sec at 14,000×g) and samples loaded onto 12% SDS-polyacrylamide gels for Western blot analysis. Quantity of TC10 pulled-down with the PAK-1 PBD-coupled agarose beads was assessed using a polyclonal antibody against TC10. Specific controls (GTP and GDP treated) were generated using lysates from unstimulated adipocytes from pair-fed rats according to manufacturer's instructions (data not shown).

Actin Polymerization Assay

The quantity of F-actin in cells was assessed using a G-actin/F-actin In Vivo Assay Kit (Catalog Number BK037, Cytoskeleton Inc., Denver, CO) following the manufacturer's recommended protocol, except for some adaptations required for working with adipocytes. Briefly, isolated adipocytes were counted, adjusted to a cell density of 1×10^6 cells/mL, and treated with 10 nM insulin for 0-5 min in the presence of 1 μM phalloidin to stabilize existing and insulin-stimulated F-actin. Cells were lysed with the provided lysis buffer and homogenized 8 strokes using 21G syringes at 37°C. The lysates were centrifuged 100,000×g for 60 min at 37°C. The supernatant (containing globular actin) was removed and the pellets (containing F- actin) was resuspended in 500 μL water with 2 μM cytochalasin D and were incubated on ice for 60 min. To aid in resuspension, samples were sheared using $26^{5/8}$G syringes. All samples were normalized for protein prior to Western analysis.

Data Analyses

Due to limitations in the amount of tissue available from each animal, assays were conducted on adipocytes isolated from multiple feeding trials. Values reported are means ± SEM. Statistical analyses were performed using either one-way ANOVA and differences between groups determined by the Tukey-Kramer multiple comparisons test (GraphPad™ InStat®; San Diego, CA), or the general linear models program on the SAS statistical package for personal computers and differences between groups determined by least square means. Data were log transformed when necessary to produce a normal distribution.

RESULTS

Since chronic ethanol feeding impairs insulin-stimulated glucose uptake independently of the PI3K pathway (41), we examined the effects of chronic ethanol feeding on insulin regulation of the Cbl/TC10 pathway. Adipocytes isolated from ethanol- and pair-fed rats were treated with or without 10 nM insulin for 90 seconds. cCbl was immunoprecipitated from the lysates, and cCbl tyrosine phosphorylation measured with an anti-phosphotyrosine antibody. Insulin rapidly increased the phosphorylation of cCbl (Figure 1A) in adipocytes isolated from pair-fed rats. Chronic ethanol feeding abolished insulin-stimulated cCbl phosphorylation (Figure 1A). Impaired insulin-stimulated cCbl tyrosine phosphorylation was not due to a reduction in cCbl expression, as there was no difference in total cCbl protein between adipocytes from pair- and ethanol-fed rats. The impaired insulin-stimulated tyrosine phosphorylation of cCbl was not due to a more general decrease in the ability of insulin to activate the insulin receptor tyrosine kinase domain as insulin receptor autophosphorylation was maintained after chronic ethanol feeding (Figure 1B). Consistent with a specific impairment in cCbl phosphorylation, the PI3K-dependent phosphorylation of Akt/PKB was unaffected by chronic ethanol feeding (Figure 1B) (41).

Phosphorylated cCbl migrates to the lipid raft microdomains in the plasma membrane after insulin stimulation (5;6;23). If chronic ethanol decreases cCbl phosphorylation, then we would expect to see reduced recruitment of cCbl to the lipid raft. To test this hypothesis, isolated adipocytes were treated with or without 10 nM insulin for 0-5 min and lysed with Triton X-100 lysis buffer. The Triton-insoluble fraction of cells, which has been described as containing lipid raft microdomains of the plasma membrane (31), was collected by centrifugation and dissolved with 60 mM OTG. cCbl was readily detected in Triton-soluble fractions from both pair- and ethanol-fed rats. In adipocytes from pair-fed rats, cCbl was not detectable in the Triton-insoluble fraction in the absence of insulin (Figure 2). In response to insulin, cCbl appears in the Triton-insoluble fraction of the adipocyte after 2 min of stimulation and is undetectable after 5 min of insulin stimulation (Figure 2). In contrast, cCbl was absent from Triton-insoluble fractions obtained from ethanol-fed rats, both with and without insulin treatment (Figure 2).

Antibodies against caveolin and transferrin receptor were used as controls for the isolation method and indicators of lipid raft integrity. The transferrin receptor, used as a marker for non-lipid raft, was only detected in the Triton-soluble portion of the cell (Figure 3). Caveolin, used as a marker for lipid rafts, was enriched in the Triton-insoluble fraction (Figure 3). Chronic ethanol feeding had no affect on the separation of these markers, indicating that the integrity of lipid rafts during isolation was similar between adipocytes from pair- and ethanol-fed rats. Taken together, these data suggest chronic ethanol feeding in rats impairs cCbl phosphorylation with an associated reduction of cCbl recruitment to the Triton-insoluble fraction of adipocytes.

Insulin-stimulated of TC10 requires cCbl phosphorylation and migration to the lipid raft (6). Since chronic ethanol feeding impairs cCbl movement to the lipid raft, we asked whether chronic ethanol feeding affects the distribution of other proteins involved in the Cbl/TC10 pathway (i.e. insulin receptor, APS, and TC10) between lipid raft and non-lipid raft fractions of the cell. Neither the insulin receptor β subunit nor APS was detectable in Triton-insoluble fractions isolated from pair- or ethanol-fed rats either at baseline or after 2 and 5 min insulin treatment (Figure 3). These data complement other studies which suggest a physical segregation between the two signaling pathways involved in insulin-stimulated glucose transport (5;6;55). Insulin stimulation markedly increased lipid raft-associated TC10 (Figure 3). There was no detectable decrease in TC10 quantity in the Triton-soluble fraction of the cell, suggesting that only a relatively small portion of TC10 translocates to lipid rafts in response to insulin (Figure 3). In adipocytes from ethanol-fed rats, there was no detectable TC10 found in Triton-insoluble fractions either with or without insulin treatment. The absence of TC10 in the Triton-insoluble fractions after insulin stimulation was not due to decreased TC10 expression, since the amount of TC10 in the Triton-soluble fraction was unchanged by chronic ethanol feeding. These data suggest that, rather than decreasing TC10 expression, chronic ethanol feeding impairs the recruitment of TC10 to the lipid raft in response to insulin stimulation.

To further characterize the effects of chronic ethanol on localization of TC10, PM fractions were prepared from isolated adipocytes and subjected to the Triton X-100 detergent extraction procedure to separate lipid raft and non-lipid raft domains specific to the PM. In the PM fractions, caveolin was enriched in the Triton-insoluble fraction, while the insulin receptor was only detectable in the Triton-soluble fraction (Figure 4), similar to their distribution in the whole cell preparations (Figure 3). In 3T3L1 cells overexpressing human or murine TC10 isoforms, TC10 was constitutively resident in lipid rafts (7;55). However, in primary rat adipocytes, only a relatively small quantity of TC10 was detected in the Triton-insoluble PM (lipid raft) fractions in untreated adipocytes (Figure 4). There was no difference in baseline quantity or localization of TC10 between pair- and ethanol-fed rats (Figure 4). Treatment with insulin resulted in a rapid increase in TC10 in the Triton-insoluble PM fraction in adipocytes from pair-fed rats (Figure 4). In contrast, after chronic ethanol feeding, insulin treatment did not increase the amount of TC10 associated with lipid raft domains in the PM (Figure 4).

Since insulin-stimulated cCbl and TC10 recruitment to the lipid raft are impaired after chronic ethanol feeding, we would expect to see a loss in insulin-stimulated TC10 activation in ethanol-fed rats. The relative amounts of active/GTP-bound TC10 in pair- and ethanol-fed rats were measured using a GST-PAK-1 PBD pull-down assay kit. Activation of TC10 was increased more than 4-fold after 5 min of insulin stimulation in adipocytes from pair-fed rats compared to unstimulated pair-fed adipocytes (Figure 5). In contrast, after chronic ethanol feeding, the amount of activated TC10 present in adipocytes not treated with insulin was 13-fold higher than in adipocytes from pair-fed rats, despite no change in total TC10 protein with chronic ethanol feeding (Figure 5). Stimulation with insulin failed to increase the amount of activated TC10 in ethanol-fed rats (Figure 5). To ensure that a lack of insulin response in ethanol-fed adipocytes was not due to a saturation of the PAK-1 PBD agarose beads at the high level of

activation seen after ethanol feeding, we conducted control experiments using only 1/6th the amount of protein in the pull-down assay. Even with the lower input of protein into the assay, we were unable to detect an increase in GTP-bound TC10 after insulin-stimulation after chronic ethanol feeding (data not shown).

Insulin acts via TC10 to modulate actin polymerization, which is required for insulin-stimulated GLUT4 translocation and glucose uptake (18;38;52). Since chronic ethanol exposure affects TC10 recruitment to lipid rafts and dysregulates the activation/inactivation cycle of TC10, we asked whether chronic ethanol feeding also impaired insulin-stimulated actin polymerization. Adipocytes from pair- and ethanol-fed rats were isolated and treated with or without 10 nM insulin for 0-5 min. Filamentous actin (F-actin) was separated from globular actin by differential centrifugation and the quantity of F-actin in each sample was determined by Western analysis. As expected, the quantity of F-actin was low in adipocytes from pair-fed rats, with a rapid increase in F-actin in response to insulin (Figure 6). In contrast, after chronic ethanol feeding, F-actin quantity was already greater than in cells from pair-fed rats at baseline, and there was no further polymerization after insulin treatment. Increased F-actin after ethanol feeding was not due to increased expression of total actin; rather, chronic ethanol feeding shifted the proportion of F-actin to total actin within the adipocyte. The increase in F-actin at baseline after chronic ethanol feeding is consistent with an increase in active TC10 at baseline in these cells. Additionally, the failure of insulin to further activate TC10 after chronic ethanol feeding parallels the inability of insulin to further stimulate actin polymerization in adipocytes from ethanol-fed rats.

DISCUSSION

Chronic ethanol feeding in rats suppresses insulin-stimulated glucose transport in adipocytes (58). This insensitivity to insulin after chronic ethanol is independent of an effect of chronic ethanol on PI3K or Akt/PKB (41). In light of recent studies suggesting the involvement of a second signaling cascade, the Cbl/TC10 pathway, in insulin-stimulated glucose uptake in adipocytes, we hypothesized that this pathway may be a target for chronic ethanol. Here we report that chronic ethanol feeding suppressed insulin-stimulated cCbl phosphorylation and caused a dysregulation of TC10 activation with an associated inhibition in actin polymerization. Impaired activation of the Cbl/TC10 pathway and actin polymerization in response to insulin was associated with decreased insulin-stimulated glucose uptake in adipocytes after chronic ethanol feeding (58). While still controversial (33), several studies have implicated the Cbl/TC10 pathway in mediating insulin-stimulated glucose transport in 3T3L1 adipocyte cultures. However, much less is known about the *in vivo* regulation of this pathway in physiological conditions of insulin resistance. The data presented here provide evidence that, under pathophysiological conditions of chronic ethanol feeding, impaired glucose transport in adipocytes is associated with decreased activity of the Cbl/TC10 pathway and dysregulation of actin polymerization.

Insulin treatment increased the tyrosine phosphorylation of cCbl in isolated rat adipocytes (Figure 1), similar to the response observed in 3T3L1 adipocytes (28). However, after chronic ethanol feeding, insulin treatment did not stimulate cCbl phosphorylation in isolated rat adipocytes. Impaired insulin-stimulated cCbl phosphorylation was independent of any decrease in total cCbl protein after chronic ethanol feeding (Figure 1). Further, this insensitivity to insulin was specific to cCbl phosphorylation, as chronic ethanol had no effect on insulin receptor autophosphorylation or serine phosphorylation of Akt/PKB (Figure 1) (41). These findings suggest that chronic ethanol feeding may specifically impair the ability of cCbl to associate with the insulin receptor, rather than generally suppressing insulin receptor tyrosine kinase activity. The adaptor protein APS is required for cCbl tyrosine phosphorylation by the insulin receptor. While chronic ethanol feeding did not change the level of APS expression in

adipocytes (Figure 3), it is possible that ethanol disrupts the function of APS and/or another required adaptor protein, CAP, thus impairing the ability of the insulin receptor to interact with and phosphorylate cCbl.

Chronic ethanol feeding impaired cCbl recruitment to the lipid raft in isolated adipocytes (Figure 2), a step required for TC10 activation in response to insulin (6). In studying the lipid raft-associated proteins involved in the Cbl/TC10 pathway, we expected to see TC10 localized in the lipid raft fraction at baseline, as previous studies overexpressing human and murine isoforms of TC10 in 3T3L1 cells found TC10 to be a resident protein of lipid rafts (55). These studies used confocal microscopy to visualize TC10 localization or extraction in Triton X-100, followed by sucrose density gradients, to demonstrate co-migration of TC10 with caveolin-1 (7;55). In our experiments in isolated adipocytes from pair-fed rats, using a similar detergent extraction method, we found the majority of TC10 to be associated with non-lipid raft fractions, with only a relatively small portion associated with lipid rafts (Figure 3 and 4). In these primary adipocytes, insulin stimulation caused a rapid recruitment of TC10 into the lipid raft. These differences may be the result of overexpression of exogenous TC10 in the previous studies and/or differences in the localization of endogenous TC10 between 3T3L1 adipocytes and primary adipocytes. Importantly, recruitment of TC10 to the lipid raft in response to insulin was completely prevented by chronic ethanol (Figure 3 and 4).

One mechanism by which chronic ethanol could impair recruitment of cCbl and TC10 to the lipid raft would be via a disruption in the integrity of the lipid raft, either in the adipocyte itself and/or during the isolation procedure. However, this mechanism seems unlikely since the distribution of caveolin, a marker for the lipid raft domain, and the transferrin receptor, a marker for non-lipid raft plasma membrane domains, between Triton-soluble and insoluble fractions were not affected by chronic ethanol feeding (Figure 3). Instead, it is more likely that chronic ethanol disrupts the molecular mechanisms mediating the regulated movement of proteins into and out of the lipid raft. While it is clear from a number of studies in various cell types that ethanol can disrupt membrane protein trafficking (reviewed in (36)), very little information is available about the potential specific effects of ethanol on recruitment of proteins to specific microdomains, such as lipid rafts, within the plasma membrane. Our data suggest that movement of proteins to lipid raft domains in response to insulin may be an important target of ethanol action in adipocytes.

Since chronic ethanol feeding impaired insulin-stimulated cCbl tyrosine phosphorylation, as well as the recruitment of cCbl and TC10 to the lipid raft, we expected to see decreased activation of TC10. Surprisingly, we found a dramatic increase in the amount of active TC10 after chronic ethanol feeding in the absence of insulin (Figure 5). The cycling between the GTP- and GDP-bound forms of a GTPase is critical to its function. A number of studies in other cell types have identified small GTP binding proteins as targets of ethanol action, consistent with the increase in the active form of TC10 after chronic ethanol feeding in the current study. For example, ethanol exposure increases the GTP-bound forms of several GTPases (10;29;42;48) including ras in mouse liver (15), RhoA in fetal rat astrocytes (10), cdc42 in SVEC4-10 cells (42), and RhoA and cdc42 *in vitro* (48).

Numerous studies have shown that the actin cytoskeleton is required for glucose uptake in adipocytes (12;38;40;52). Since the Cbl/TC10 pathway has been implicated in the process of cortical actin reorganization at the plasma membrane (7), we hypothesized that actin polymerization might be a downstream event in this pathway targeted by chronic ethanol feeding. After chronic ethanol feeding, F-actin quantity was increased even in the absence of insulin, consistent with the greater quantity of TC10 found in the active/GTP-bound form (Figures 5 and 6). Further, insulin-stimulated actin polymerization was inhibited by chronic ethanol exposure (Figure 6), again consistent with impaired activation of TC10 by insulin in

adipocytes from ethanol-fed rats. These data are consistent with a recent study showing constitutively active TC10 completely disrupts adipocyte cortical actin when expressed in 3T3L1 cells (21).

A number of studies describe the development of insulin resistance during chronic ethanol exposure in humans and rodent models (9;19;39;46;51). While chronic ethanol feeding suppresses insulin-stimulated glucose transport in isolated rat adipocytes (41;58), it is not yet known whether impaired glucose transport in adipocytes contributes to insulin resistance in the intact organism. Recently, two groups have carried out hyperinsulinemic-euglycemic clamp studies in rats chronically exposed to ethanol (39;51). Both groups found that chronic ethanol exposure both increased hepatic glucose production, associated with hepatic insulin resistance, and decreased glucose utilization rates. However, neither study addressed the specific contributions of adipose tissue and/or skeletal muscle to impaired glucose disposal *in vivo* after chronic ethanol feeding. Despite the relatively minor contribution of adipose tissue relative to skeletal muscle in mediating whole body glucose disposal, studies in transgenic animals indicate that glucose transport capacity in adipose tissue can make significant contributions to whole body insulin sensitivity. For example, adipocyte-specific GLUT4-/- mice develop insulin resistance and glucose intolerance (32), while mice with adipose-specific overexpression of GLUT4 have enhanced insulin sensitivity (47). These studies suggest that impaired insulin-stimulated glucose uptake by adipose can contribute to a secondary insulin resistance in both skeletal muscle and liver (32). Studies are currently underway to determine the impact of impaired insulin-stimulated glucose uptake in adipocytes on *in vivo* insulin sensitivity in rats chronically fed ethanol.

In summary, we have identified the Cbl/TC10 pathway as a target for chronic ethanol action in rat adipocytes. Chronic ethanol feeding decreased insulin-stimulated tyrosine phosphorylation of cCbl, disrupted the recruitment of cCbl and TC10 to lipid raft microdomains, caused a marked increase in GTP-bound (active state) TC10 and inhibited insulin-stimulated actin polymerization. These data identify the Cbl/TC10 pathway as a specific target of ethanol action and suggest an association between disruption of the Cbl/TC10 pathway under pathophysiological situations, such as chronic alcohol consumption, and impaired insulin-stimulated glucose uptake in adipocytes.

Reference List

1. Ahmed Z, Pillay TS. Adapter protein with a pleckstrin homology (PH) and an Src homology 2 (SH2) domain (APS) and SH2-B enhance insulin-receptor autophosphorylation, extracellular-signal-regulated kinase and phosphoinositide 3-kinase-dependent signalling. Biochem J 2003;371:405–12. [PubMed: 12521378]
2. Avogaro A, Tiengo A. Alcohol, glucose metabolism and diabetes. Diabetes Metab Rev 1993;9:129–46. [PubMed: 8258307]
3. Bandyopadhyay G, Standaert ML, Galloway L, Moscat J, Farese RV. Evidence for involvement of protein kinase C (PKC)-zeta and noninvolvement of diacylglycerol-sensitive PKCs in insulin-stimulated glucose transport in L6 myotubes. Endocrinology 1997;138:4721–31. [PubMed: 9348199]
4. Bandyopadhyay G, Standaert ML, Zhao L, Yu B, Avignon A, Galloway L, Karnam P, Moscat J, Farese RV. Activation of protein kinase C (alpha, beta, and zeta) by insulin in 3T3/L1 cells. Transfection studies suggest a role for PKC-zeta in glucose transport. J Biol Chem 1997;272:2551–8. [PubMed: 8999972]
5. Baumann CA, Ribon V, Kanzaki M, Thurmond DC, Mora S, Shigematsu S, Bickel PE, Pessin JE, Saltiel AR. CAP defines a second signalling pathway required for insulin-stimulated glucose transport. Nature 2000;407:202–7. [PubMed: 11001060]
6. Chiang SH, Baumann CA, Kanzaki M, Thurmond DC, Watson RT, Neudauer CL, Macara IG, Pessin JE, Saltiel AR. Insulin-stimulated GLUT4 translocation requires the CAP-dependent activation of TC10. Nature 2001;410:944–8. [PubMed: 11309621]

7. Chiang SH, Hou JC, Hwang J, Pessin JE, Saltiel AR. Cloning and functional characterization of related TC10 isoforms, a subfamily of Rho proteins involved in insulin-stimulated glucose transport. J Biol Chem 2002;277:13067–73. [PubMed: 11821390]
8. Farese RV. Function and dysfunction of aPKC isoforms for glucose transport in insulin-sensitive and insulin-resistant states. Am J Physiol Endocrinol Metab 2002;283:E1–11. [PubMed: 12067836]
9. Forman DT. The effect of ethanol and its metabolites on carbohydrate, protein, and lipid metabolism. Ann Clin Lab Sci 1988;18:181–9. [PubMed: 3291739]
10. Guasch RM, Tomas M, Minambres R, Valles S, Renau-Piqueras J, Guerri C. RhoA and lysophosphatidic acid are involved in the actin cytoskeleton reorganization of astrocytes exposed to ethanol. J Neurosci Res 2003;72:487–502. [PubMed: 12704810]
11. Guilherme A, Czech MP. Stimulation of IRS-1-associated phosphatidylinositol 3-kinase and Akt/protein kinase B but not glucose transport by beta1-integrin signaling in rat adipocytes. J Biol Chem 1998;273:33119–22. [PubMed: 9837876]
12. Guilherme A, Emoto M, Buxton JM, Bose S, Sabini R, Theurkauf WE, Leszyk J, Czech MP. Perinuclear localization and insulin responsiveness of GLUT4 requires cytoskeletal integrity in 3T3-L1 adipocytes. J Biol Chem 2000;275:38151–9. [PubMed: 10950952]
13. Inoue M, Chang L, Hwang J, Chiang SH, Saltiel AR. The exocyst complex is required for targeting of Glut4 to the plasma membrane by insulin. Nature 2003;422:629–33. [PubMed: 12687004]
14. Isakoff SJ, Taha C, Rose E, Marcusohn J, Klip A, Skolnik EY. The inability of phosphatidylinositol 3-kinase activation to stimulate GLUT4 translocation indicates additional signaling pathways are required for insulin-stimulated glucose uptake. Proc Natl Acad Sci U S A 1995;92:10247–51. [PubMed: 7479761]
15. Isayama F, Froh M, Yin M, Conzelmann LO, Milton RJ, McKim SE, Wheeler MD. TNF alpha-induced Ras activation due to ethanol promotes hepatocyte proliferation independently of liver injury in the mouse. Hepatology 2004;39:721–31. [PubMed: 14999690]
16. JeBailey L, Rudich A, Huang X, Di Ciano-Oliveira C, Kapus A, Klip A. Skeletal muscle cells and adipocytes differ in their reliance on TC10 and Rac for insulin-induced actin remodeling. Mol Endocrinol 2004;18:359–72. [PubMed: 14615606]
17. Jiang T, Sweeney G, Rudolf MT, Klip A, Traynor-Kaplan A, Tsien RY. Membrane-permeant esters of phosphatidylinositol 3,4,5-trisphosphate. J Biol Chem 1998;273:11017–24. [PubMed: 9556583]
18. Jiang ZY, Chawla A, Bose A, Way M, Czech MP. A phosphatidylinositol 3-kinase-independent insulin signaling pathway to N-WASP/Arp2/3/F-actin required for GLUT4 glucose transporter recycling. J Biol Chem 2002;277:509–15. [PubMed: 11694514]
19. Jose Gerard M, Klatsky AL, Siegelaub AB, Friedman GD, Feldman R. Serum glucose levels and alcohol-consumption habits in a large population. Diabetes 1977;26:780–5. [PubMed: 885299]
20. Kanzaki M, Pessin JE. Insulin-stimulated GLUT4 translocation in adipocytes is dependent upon cortical actin remodeling. J Biol Chem 2001;276:42436–44. [PubMed: 11546823]
21. Kanzaki M, Watson RT, Hou JC, Stamnes M, Saltiel AR, Pessin JE. Small GTP-binding protein TC10 differentially regulates two distinct populations of filamentous actin in 3T3L1 adipocytes. Mol Biol Cell 2002;13:2334–46. [PubMed: 12134073]
22. Kao WH, Puddey IB, Boland LL, Watson RL, Brancati FL. Alcohol consumption and the risk of type 2 diabetes mellitus: atherosclerosis risk in communities study. Am J Epidemiol 2001;154:748–57. [PubMed: 11590088]
23. Kimura A, Baumann CA, Chiang SH, Saltiel AR. The sorbin homology domain: a motif for the targeting of proteins to lipid rafts. Proc Natl Acad Sci U S A 2001;98:9098–103. [PubMed: 11481476]
24. Knudsen BS, Feller SM, Hanafusa H. Four proline-rich sequences of the guanine-nucleotide exchange factor C3G bind with unique specificity to the first Src homology 3 domain of Crk. J Biol Chem 1994;269:32781–7. [PubMed: 7806500]
25. Kohn AD, Summers SA, Birnbaum MJ, Roth RA. Expression of a constitutively active Akt Ser/Thr kinase in 3T3-L1 adipocytes stimulates glucose uptake and glucose transporter 4 translocation. J Biol Chem 1996;271:31372–8. [PubMed: 8940145]
26. Krook A, Whitehead JP, Dobson SP, Griffiths MR, Ouwens M, Baker C, Hayward AC, Sen SK, Maassen JA, Siddle K, Tavare JM, O'Rahilly S. Two naturally occurring insulin receptor tyrosine kinase domain mutants provide evidence that phosphoinositide 3-kinase activation alone is not

sufficient for the mediation of insulin's metabolic and mitogenic effects. J Biol Chem 1997;272:30208–14. [PubMed: 9374504]

27. Lee J, Pilch PF. The insulin receptor: structure, function, and signaling. Am J Physiol 1994;266:C319–34. [PubMed: 8141246]
28. Liu J, Kimura A, Baumann CA, Saltiel AR. APS facilitates c-Cbl tyrosine phosphorylation and GLUT4 translocation in response to insulin in 3T3-L1 adipocytes. Mol Cell Biol 2002;22:3599–609. [PubMed: 11997497]
29. Marmillot P, Rao MN, Lakshman MR. Chronic ethanol exposure in rats affects rabs-dependent hepatic trafficking of apolipoprotein E and transferrin. Alcohol 2001;25:195–200. [PubMed: 11839466]
30. Martin SS, Haruta T, Morris AJ, Klippel A, Williams LT, Olefsky JM. Activated phosphatidylinositol 3-kinase is sufficient to mediate actin rearrangement and GLUT4 translocation in 3T3-L1 adipocytes. J Biol Chem 1996;271:17605–8. [PubMed: 8663595]
31. Mastick CC, Saltiel AR. Insulin-stimulated tyrosine phosphorylation of caveolin is specific for the differentiated adipocyte phenotype in 3T3-L1 cells. J Biol Chem 1997;272:20706–14. [PubMed: 9252391]
32. Minokoshi Y, Kahn CR, Kahn BB. Tissue-specific ablation of the GLUT4 glucose transporter or the insulin receptor challenges assumptions about insulin action and glucose homeostasis. J Biol Chem 2003;278:33609–12. [PubMed: 12788932]
33. Mitra P, Zheng X, Czech MP. RNAi-based analysis of CAP, Cbl, and CrkII function in the regulation of GLUT4 by insulin. J Biol Chem 2004;279:37431–5. [PubMed: 15258163]
34. Moodie SA, Alleman-Sposeto J, Gustafson TA. Identification of the APS protein as a novel insulin receptor substrate. J Biol Chem 1999;274:11186–93. [PubMed: 10196204]
35. Myers MG Jr, Backer JM, Sun XJ, Shoelson S, Hu P, Schlessinger J, Yoakim M, Schaffhausen B, White MF. IRS-1 activates phosphatidylinositol 3'-kinase by associating with src homology 2 domains of p85. Proc Natl Acad Sci U S A 1992;89:10350–4. [PubMed: 1332046]
36. Nagy LE, Lakshman MR, Casey CA, Bearer CF. Ethanol and membrane protein trafficking: diverse mechanisms of ethanol action. Alcohol Clin Exp Res 2002;26:287–93. [PubMed: 11964570]
37. Nave BT, Haigh RJ, Hayward AC, Siddle K, Shepherd PR. Compartment-specific regulation of phosphoinositide 3-kinase by platelet-derived growth factor and insulin in 3T3-L1 adipocytes. Biochem J 1996;318:55–60. [PubMed: 8761452]
38. Omata W, Shibata H, Li L, Takata K, Kojima I. Actin filaments play a critical role in insulin-induced exocytotic recruitment but not in endocytosis of GLUT4 in isolated rat adipocytes. Biochem J 346 Pt 2000;2:321–8. [PubMed: 10677349]
39. Onishi Y, Honda M, Ogihara T, Sakoda H, Anai M, Fujishiro M, Ono H, Shojima N, Fukushima Y, Inukai K, Katagiri H, Kikuchi M, Oka Y, Asano T. Ethanol feeding induces insulin resistance with enhanced PI 3-kinase activation. Biochem Biophys Res Commun 2003;303:788–94. [PubMed: 12670480]
40. Patki V, Buxton J, Chawla A, Lifshitz L, Fogarty K, Carrington W, Tuft R, Corvera S. Insulin action on GLUT4 traffic visualized in single 3T3-l1 adipocytes by using ultra-fast microscopy. Mol Biol Cell 2001;12:129–41. [PubMed: 11160828]
41. Poirier LA, Rachdaoui N, Nagy LE. GLUT4 vesicle trafficking in rat adipocytes after ethanol feeding: regulation by heterotrimeric G-proteins. Biochem J 2001;354:323–30. [PubMed: 11171110]
42. Qian Y, Luo J, Leonard SS, Harris GK, Millecchia L, Flynn DC, Shi X. Hydrogen peroxide formation and actin filament reorganization by Cdc42 are essential for ethanol-induced in vitro angiogenesis. J Biol Chem 2003;278:16189–97. [PubMed: 12598535]
43. Rachdaoui N, Sebastian BM, Nagy LE. Chronic ethanol feeding impairs endothelin-1-stimulated glucose uptake via decreased G alpha 11 expression in rat adipocytes. Am J Physiol Endocrinol Metab 2003;285:E303–10. [PubMed: 12684223]
44. Ribon V, Saltiel AR. Insulin stimulates tyrosine phosphorylation of the protooncogene product of c-Cbl in 3T3-L1 adipocytes. Biochem J 1997;324:839–45. [PubMed: 9210408]
45. Saltiel AR, Pessin JE. Insulin signaling in microdomains of the plasma membrane. Traffic 2003;4:711–6. [PubMed: 14617354]

46. Selby JV, Newman B, King MC, Friedman GD. Environmental and behavioral determinants of fasting plasma glucose in women. A matched co-twin analysis. Am J Epidemiol 1987;125:979–88. [PubMed: 3578256]
47. Shepherd PR, Gnudi L, Tozzo E, Yang H, Leach F, Kahn BB. Adipose cell hyperplasia and enhanced glucose disposal in transgenic mice overexpressing GLUT4 selectively in adipose tissue. J Biol Chem 1993;268:22243–6. [PubMed: 8226728]
48. Slater SJ, Cook AC, Seiz JL, Malinowski SA, Stagliano BA, Stubbs CD. Effects of ethanol on protein kinase C alpha activity induced by association with Rho GTPases. Biochemistry 2003;42:12105–14. [PubMed: 14556642]
49. Staubs PA, Nelson JG, Reichart DR, Olefsky JM. Platelet-derived growth factor inhibits insulin stimulation of insulin receptor substrate-1-associated phosphatidylinositol 3-kinase in 3T3-L1 adipocytes without affecting glucose transport. J Biol Chem 1998;273:25139–47. [PubMed: 9737973]
50. Tanti JF, Grillo S, Gremeaux T, Coffer PJ, Van Obberghen E, Le Marchand-Brustel Y. Potential role of protein kinase B in glucose transporter 4 translocation in adipocytes. Endocrinology 1997;138:2005–10. [PubMed: 9112399]
51. Wan Q, Liu Y, Guan Q, Gao L, Lee KO, Zhao J. Ethanol feeding impairs insulin-stimulated glucose uptake in isolated rat skeletal muscle: role of Gs alpha and cAMP. Alc. Clin. Expt. Res. 2005
52. Wang Q, Bilan PJ, Tsakiridis T, Hinek A, Klip A. Actin filaments participate in the relocalization of phosphatidylinositol3-kinase to glucose transporter-containing compartments and in the stimulation of glucose uptake in 3T3-L1 adipocytes. Biochem J 1998;331:917–28. [PubMed: 9560323]
53. Wang Q, Somwar R, Bilan PJ, Liu Z, Jin J, Woodgett JR, Klip A. Protein kinase B/Akt participates in GLUT4 translocation by insulin in L6 myoblasts. Mol Cell Biol 1999;19:4008–18. [PubMed: 10330141]
54. Wannamethee SG, Shaper AG, Perry IJ, Alberti KG. Alcohol consumption and the incidence of type II diabetes. J Epidemiol Community Health 2002;56:542–8. [PubMed: 12080164]
55. Watson RT, Shigematsu S, Chiang SH, Mora S, Kanzaki M, Macara IG, Saltiel AR, Pessin JE. Lipid raft microdomain compartmentalization of TC10 is required for insulin signaling and GLUT4 translocation. J Cell Biol 2001;154:829–40. [PubMed: 11502760]
56. Wei M, Gibbons LW, Mitchell TL, Kampert JB, Blair SN. Alcohol intake and incidence of type 2 diabetes in men. Diabetes Care 2000;23:18–22. [PubMed: 10857962]
57. Wiese RJ, Mastick CC, Lazar DF, Saltiel AR. Activation of mitogen-activated protein kinase and phosphatidylinositol 3'-kinase is not sufficient for the hormonal stimulation of glucose uptake, lipogenesis, or glycogen synthesis in 3T3-L1 adipocytes. J Biol Chem 1995;270:3442–6. [PubMed: 7852430]
58. Wilkes JJ, DeForrest LL, Nagy LE. Chronic ethanol feeding in a high-fat diet decreases insulin-stimulated glucose transport in rat adipocytes. Am J Physiol 1996;271:E477–84. [PubMed: 8843741]

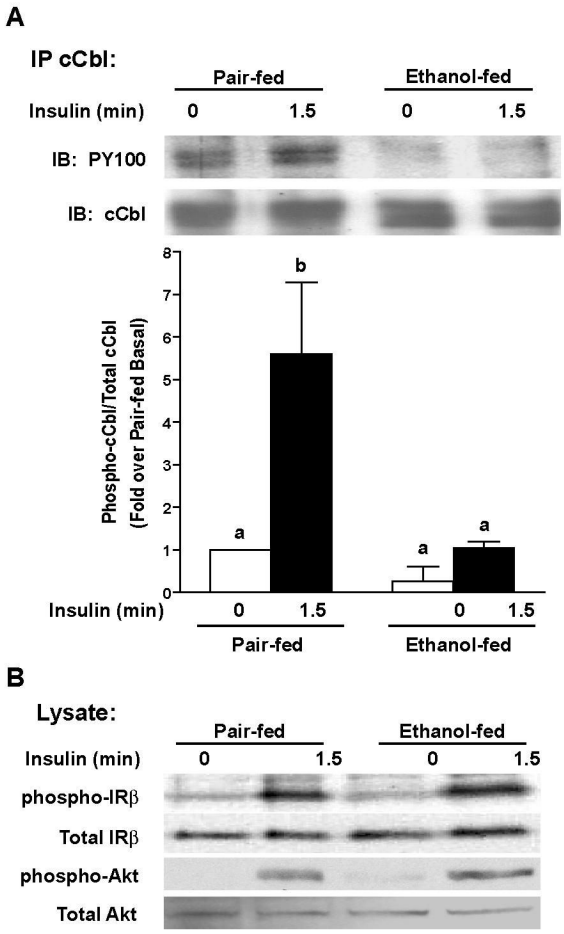

Fig. 1.

Chronic ethanol exposure impairs insulin-stimulated cCbl tyrosine phosphorylation. *A.* Isolated rat adipocytes were stimulated with or without 10 nM insulin for 0-1.5 min and lysed. Lysates were subjected to immunoprecipitation with a polyclonal antibody directed against cCbl. Samples were probed with an anti-phosphotyrosine (PY100) or anti-cCbl antibody. Representative blots are shown. Graph represents mean values ± SEM, $n = 4$. Open bars, unstimulated; solid bars, insulin-stimulated. Values with different letters are significantly different, $p < 0.05$. *B.* Isolated rat adipocytes were stimulated with or without 10 nM insulin for 0-1.5 min and lysed. Lysates were separated by SDS-PAGE and analyzed with either anti-IRβ (insulin receptor β subunit), anti-phosphotyrosine antibody (4G10; for phospho-IRβ), anti-phosphospecific-Akt/PKB, or anti-Akt/PKB.

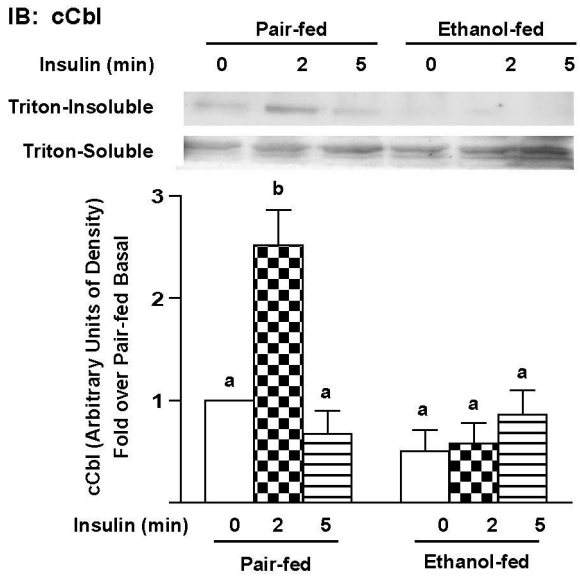

Fig. 2.

Insulin-stimulated cCbl translocation to lipid raft is inhibited by chronic ethanol feeding. Isolated adipocytes from pair- and ethanol-fed rats were incubated with or with 10 nM insulin for 0-5 min and lysed. Lysates were subjected to detergent extraction (1% Triton X-100) and Triton-insoluble fractions were solubilized with 60 mM octyl β-D-thioglucopyranoside (OTG) as described in *Experimental Procedures*. Fractions were separated by SDS-PAGE and transferred to PVDF membrane for Western blot analysis using a polyclonal anti-cCbl antibody. Representative blots are shown. Graph represents mean values ± SEM, $n = 4$. Open bars, unstimulated; checkered bars, 2 min insulin; lined bars, 5 min insulin. Values with different letters are significantly different, $p < 0.01$.

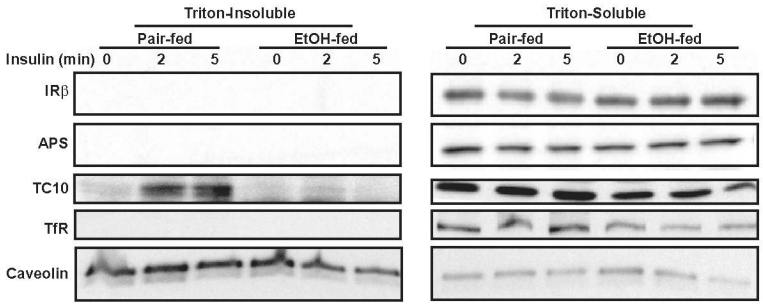

Fig. 3.

The distribution of proteins to lipid raft and non-lipid raft plasma membrane domains is disrupted by chronic ethanol feeding. Isolated adipocytes from pair- and ethanol (EtOH) fed rats, stimulated with or without 10 nM insulin for 0-5 min were lysed and Triton-soluble and —insoluble fractions were obtained as described in Experimental Procedures, and separated by SDS-PAGE for Western blot analysis. Antibodies directed against the beta subunit of the insulin receptor (IRβ), APS, TC10, transferrin receptor (TfR), or caveolin were used for ECL detection. Representative blots are shown (IRβ and APS, $n = 5$; TfR, and caveolin, $n = 4$; and TC10, n = 3).

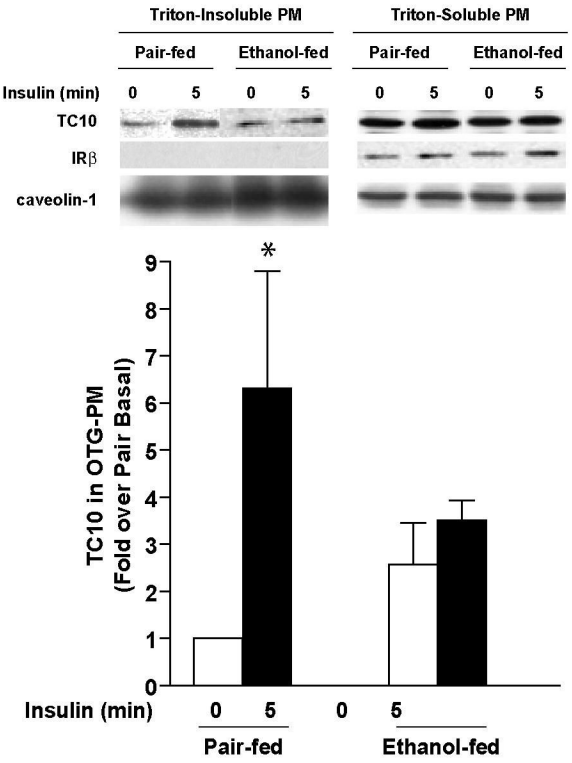

Fig. 4.

TC10 recruitment to lipid raft domains of the plasma membrane is inhibited after chronic ethanol exposure. Triton-soluble and —insoluble fractions were obtained as described in *Experimental Procedures* from plasma membrane fractions of adipocytes isolated from pair- and ethanol- (EtOH) fed rats, stimulated with or without 10 nM insulin for 0-5 min. Samples were separated by SDS-PAGE for Western analysis. Antibodies directed against the beta subunit of the insulin receptor (IRβ), TC10 or caveolin were used for ECL detection. Representative blots of three repeats are shown. Graph values are represented as the mean ± SEM of $n = 3$. Open bars, unstimulated; solid bars, insulin stimulated. *p = 0.010.

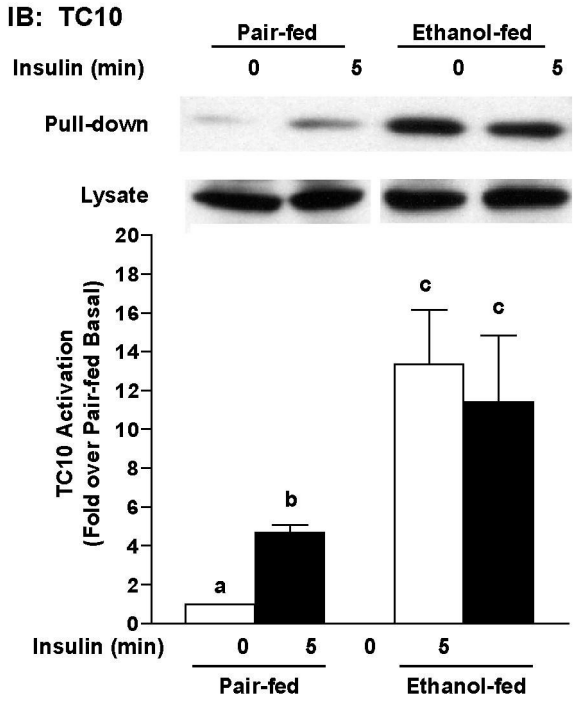

Fig. 5.

Chronic ethanol feeding interferes with TC10 activation. Adipocytes from pair- and ethanol-fed rats were isolated and incubated with or without 10 nM insulin for 0-5 min, lysed and TC10 activation was assessed using a PAK-1 PBD pull-down assay kit (Upstate) and a polyclonal antibody directed against TC10. Samples were subjected to SDS-PAGE and transferred for western analysis. Blots are representative of $n = 3$, graph shown display mean values ± SEM, $n = 3$. Open bars, unstimulated; solid bars, insulin stimulated. Values with different letters are significantly different, $p < 0.05$.

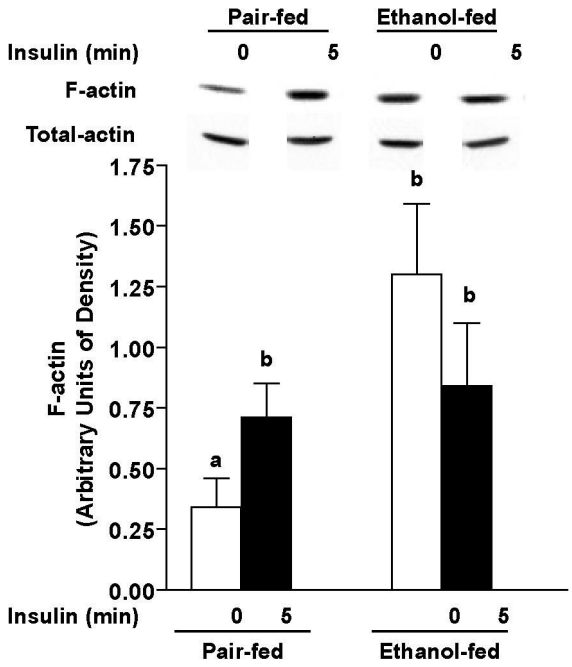

Fig. 6.

Insulin-stimulated F-actin formation is disrupted in adipocytes from chronic ethanol-fed animals. Adipocytes from pair- and ethanol-fed rats were isolated and treated with or without 10 nM insulin for 0-5 min, lysed and the relative amounts of filamentous actin assessed using a G-actin/F-actin In Vivo Assay Kit (Cytoskeleton, Inc.) as described in *Experimental Procedures*. Samples were separated by SDS-PAGE and analyzed by immunoblotting using an antibody directed against actin. Whole cell lysates were used to determine total actin. Blots are representative of six repeats and graph shown represents mean values ± SEM, n = 5-6. Open bars, unstimulated; solid bars, insulin stimulated. Values with different letters are significantly different, $p < 0.05$.